Supporting information

Depressed P3-O3' phase transition in O3-type layered cathode for advanced sodium-ion batteries

Zhaohui Liang[a], Meng Ren[a], Yihe Guo[a], Tong Zhang[a], Xiuling Gao[c], Hua Ma[c], and Fujun Li[a,b] *

[a]Key Laboratory of Advanced Energy Materials Chemistry (Ministry of Education), Renewable Energy Conversion and Storage Center (RECAST), College of Chemistry, Nankai University, Tianjin 300071, China.

[b]Haihe Laboratory of Sustainable Chemical Transformations, Tianjin 300192, China.

[c]National Enterprise Technology Center & Research Institute, Tianjin EV Energies Co., Ltd., Tianjin 300380, China

*Email: fujunli@nankai.edu.cn

Experimental section

Synthesis of materials

O3-NaNM, O3-NaNMCS, O3-NaNMC, and O3-NaNMS were prepared by solid state reaction. Stoichiometric percentage of Na_2CO_3 (99.5%), NiO (99%), MnO_2 (99%), CuO (99%) and SnO_2 (99.8%) were mixed for 6 h, and an excess of 5 mol% Na_2CO_3 was added. The mixture is then pressed into pellets under a pressure of 25 MPa, calcined in a muffler oven in air at 900 °C for 15 hours, then immediately transferred into an argon filled glove box to protect the structure from moisture in the air and quenched to room temperature under vacuum.

Materials characterization

X-ray diffraction (XRD, Rigaku SmartLab) powder measurements with Cu Kα radiation were performed to confirm the structure of the samples obtained. Rietveld refinement was conducted with the Fullprof software.[1] The VESTA software was utilized to calculate the corresponding lattice parameters of materials.[2] The elemental ratios of samples were identified by ICP-OES. The FE-SEM (JEOL JSM-7900F, AEMC) and TEM (FEI Talos F200X G2, AEMC) were applied to examine the morphology and crystal structure of samples. The charge compensation mechanism of prepared materials was revealed by X-ray photoelectron spectroscopy (XPS, ThermoFischer Nexsa). Ni K-edge, Mn K-edge and Cu K-edge were collected by *Ex-situ* XAS at Hamburger Synchrotronstrahlungslabor (Germany). The XAS data was collected under fluorescence mode and manipulated by Demeter software package.

Electrochemical measurements

The coin cell (CR2032) was assembled for all electrochemical tests within a glove box under argon atmosphere. The electrodes were prepared by coating a slurry comprised of active material (80 wt%), polyvinylidene fluoride (PVDF) binder (10 wt%), and Super P (10 wt%) in N-methyl-2-pyrrolidone (NMP) onto an aluminum foil and then drying the foil at 90°C for 12 hours under vacuum condition. For half-cells, sodium foil and glass fiber were used as the anode and the separator respectively. The electrolyte

was 1.0 M NaPF6 in propylene carbonate/ethyl methyl carbonate (PC/EMC=1:1 in volume) with 2 vol% fluoroethylene carbonate (FEC), and the loading mass of active material for each electrode was ~3.0 mg cm^{-2}. The galvanostatic charge/discharge measurements and GITT were carried out on a Land CT2001A battery test system (Land, Wuhan, China) in a voltage range of 2.0-4.0 V at room temperature. Cyclic voltammetry (CV) was carried out on a Solartron 1470E electrochemical workstation at scan rates of 0.1 mV s^{-1}. GITT was performed by applying the repeated current pulses at 10 mA g^{-1} for 30 minutes, followed by relaxation of 4 h. The diffusion coefficient of Na^+ can be calculated according to the following equation:

$$D_{Na} = \frac{4}{\pi\tau}\left(\frac{m_B V_M}{M_B S}\right)^2\left(\frac{\Delta E_s}{\Delta E_\tau}\right)^2$$

where D_{Na} is the diffusion coefficient Na^+, m_B and M_B are the mass of active material and molecular weight, respectively. V_M is the molar volume of active material, S is the area of electrode, ΔE_s and ΔE_τ represent the change in the steady-state voltage after subtracting the IR drop and transient change in voltage. The full battery was constructed by assembling O3-NaNMCS as the cathode and HC as the anode, and the capacity ratio of O3-NaNMCS/HC is around 1.1. The charge/discharge measurements of full cells were executed over a voltage range of 1.9−3.9 V at 25°C.

Density functional theory (DFT) calculations

Density functional theory (DFT) calculations were performed using Vienna ab-initio simulation package (VASP)[3] with the generalized gradient approximation (GGA) and the Perdew-Burke-Eznerhof (PBE) functional (GGA-PBE) to describe the exchange-correlation energy of electrons. The projector-augmented wave method (PAW) was used to treat the interaction between the atomic cores and electrons. The U values for Mn and Ni are set as 3.9 eV and 6.2 eV with spin polarization also considered.

We used a 3×2×2 K-point mesh to sample the reciprocal space with a cutoff energy of 450 eV for geometrical optimizations. Atomic positions and cell vectors were fully optimized until all force components were less than 0.02 eV Å-1. During density of

states (DOS) analyses, the cutoff energy is enlarged to 450 eV for higher precision, and a 4×3×3 K-point mesh is adopted.

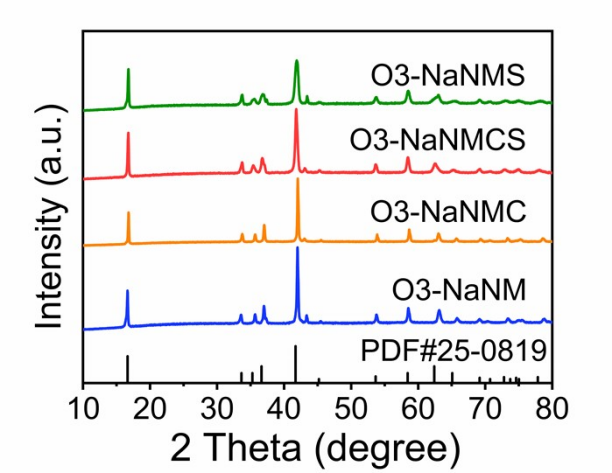

Fig. S1 Powder XRD patterns of O3-NaNM, O3-NaNMC, O3-NaNMCS, and O3-NaNMS.

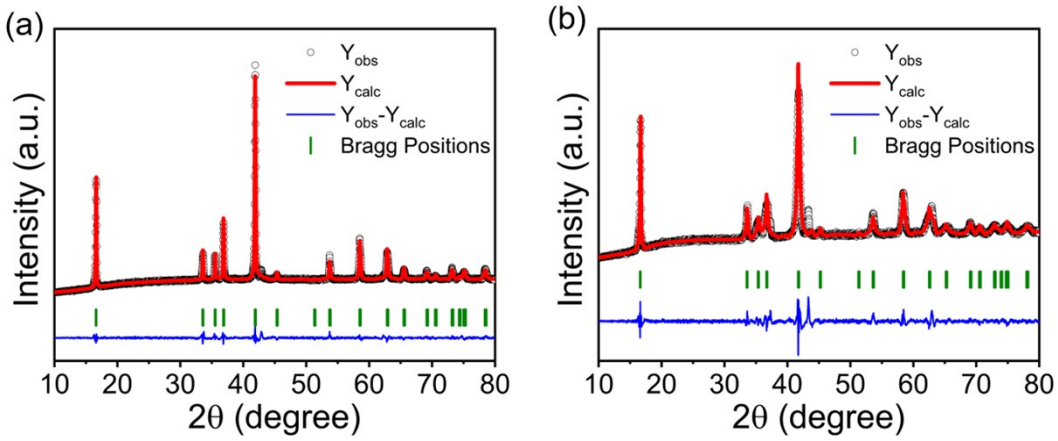

Fig. S2 XRD patterns and Rietveld refinements of (a) O3-NaNMC and (b) O3-NaNMS.

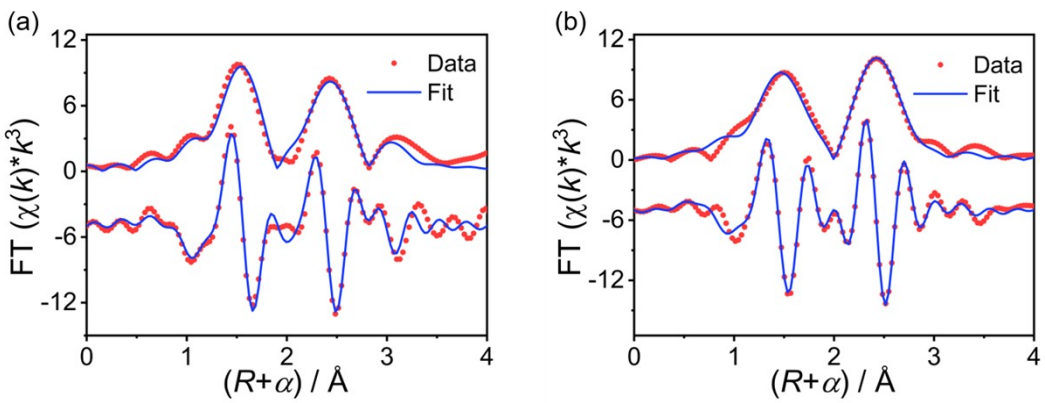

Fig. S3 (a) Ni K-edge and (b) Mn K-edge EXAFS (points) and curvefit (line) for O3-NaNM, shown in R-space (FT magnitude and imaginary component). The data are k3-weighted and not phase-corrected.

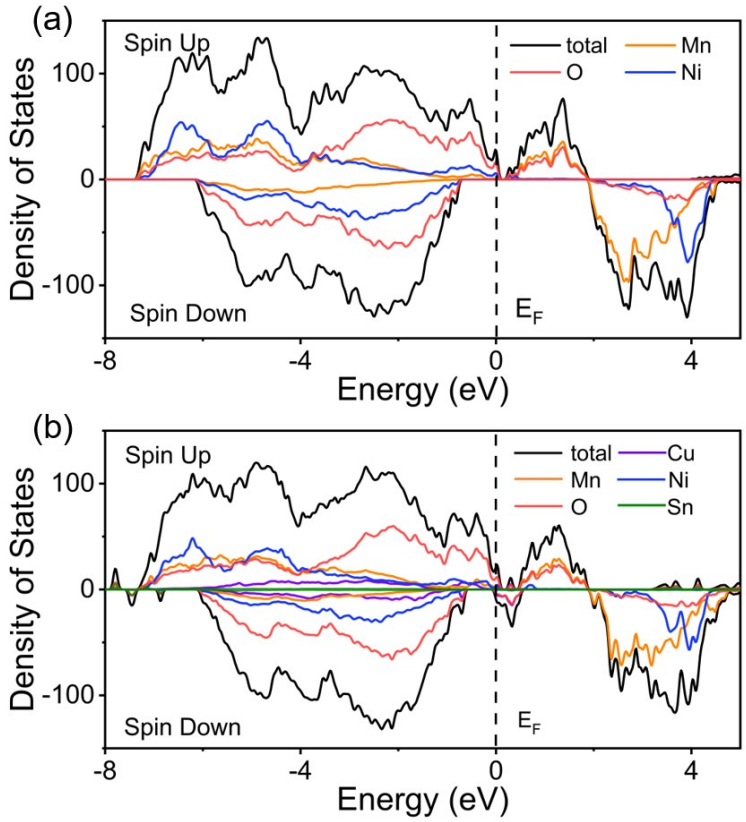

Fig. S4 Density of state (DOS) of (a) O3-NaNM and (b) O3-NaNMCS at the top and bottom, respectively.

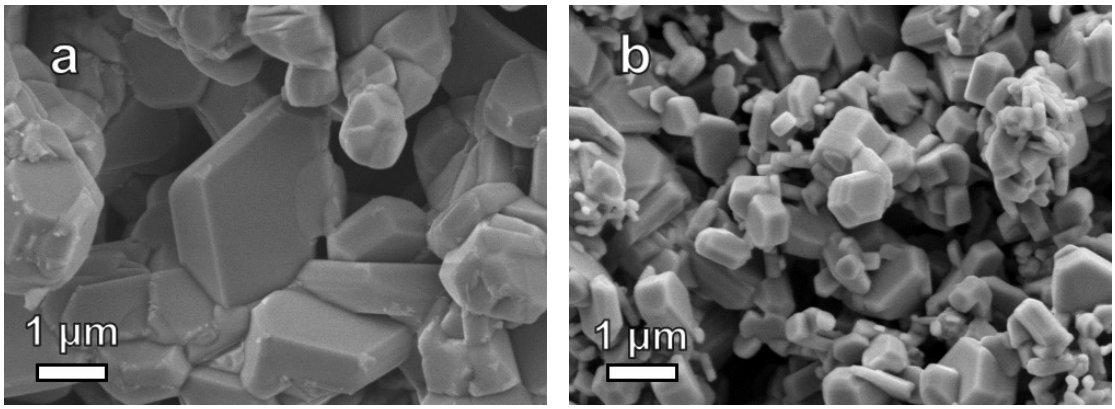

Fig. S5 SEM images of (a) O3-NaNMC and (b) O3-NaNMS.

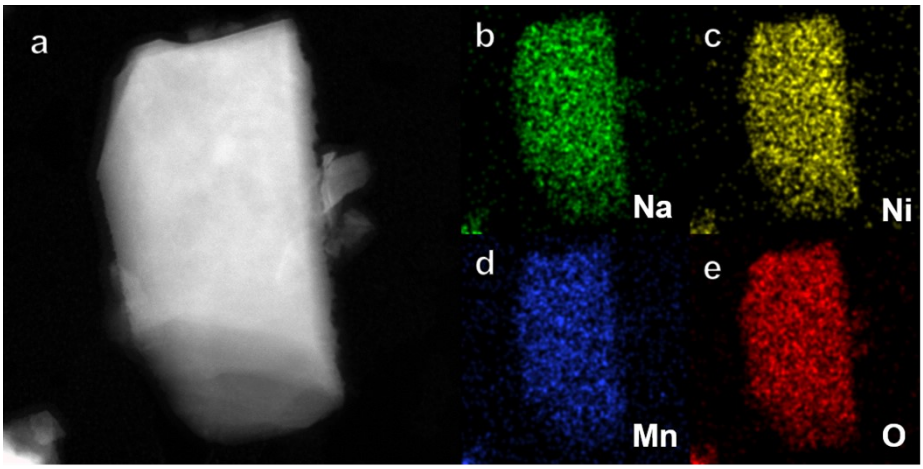

Fig. S6 (a-e) Elemental mappings of O3-NaNM.

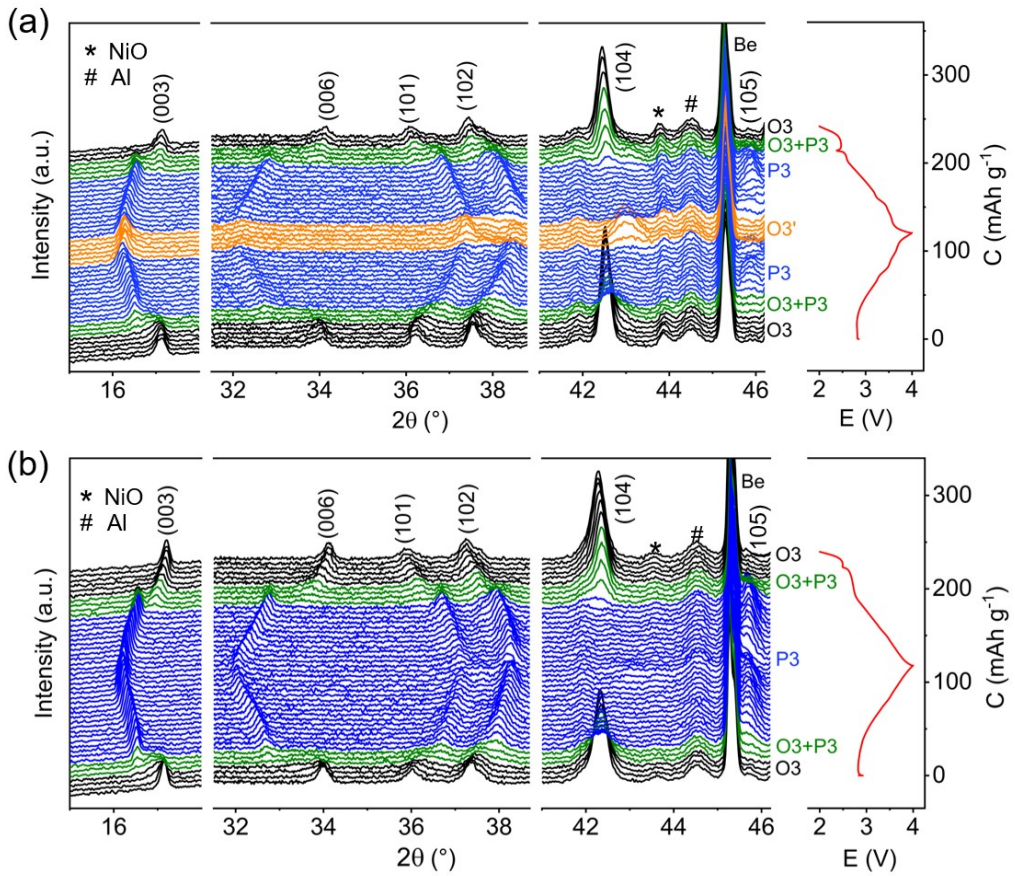

Fig. S7 *In-situ* XRD patterns of (a) O3-NaNM and (b) O3-NaNMCS between 2.0 and 4.0 V at 20 mA g^{-1}.

.

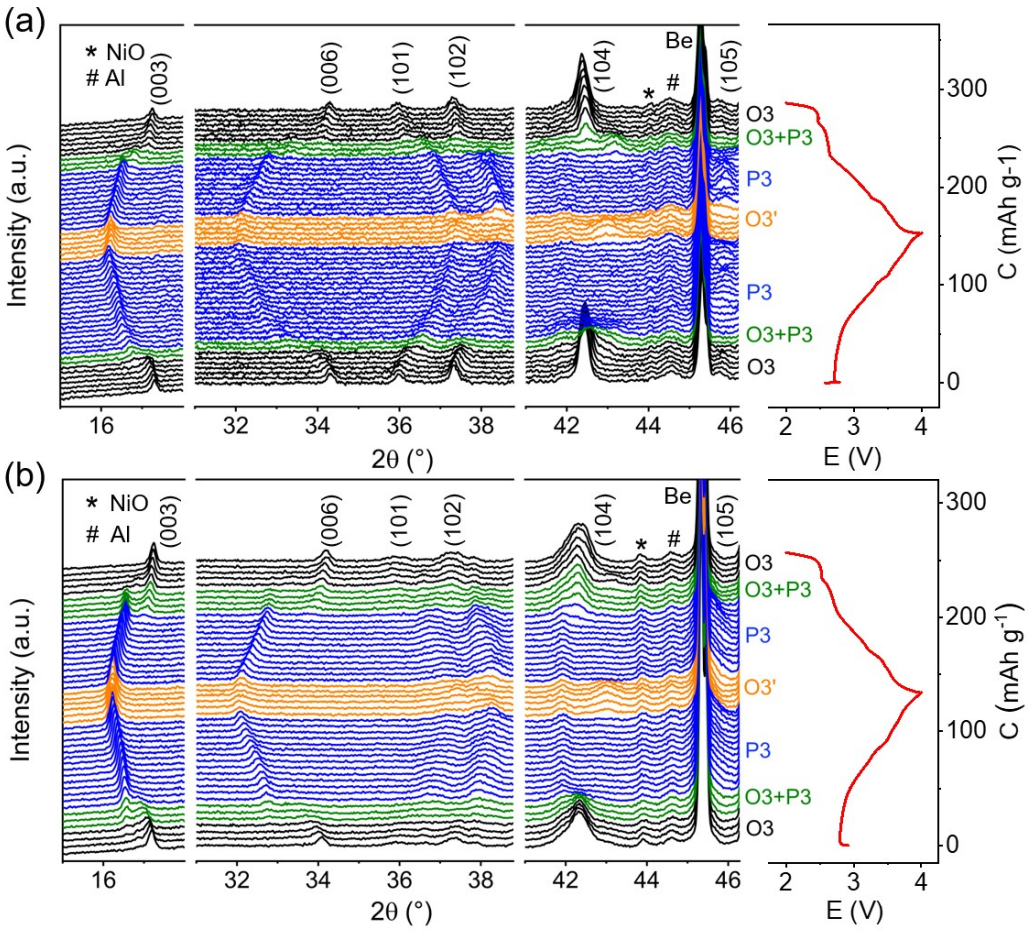

Fig. S8 *In-situ* XRD patterns of (a) O3-NaNMC and (b) O3-NaNMS between 2.0 and 4.0 V at 20 mA g^{-1}.

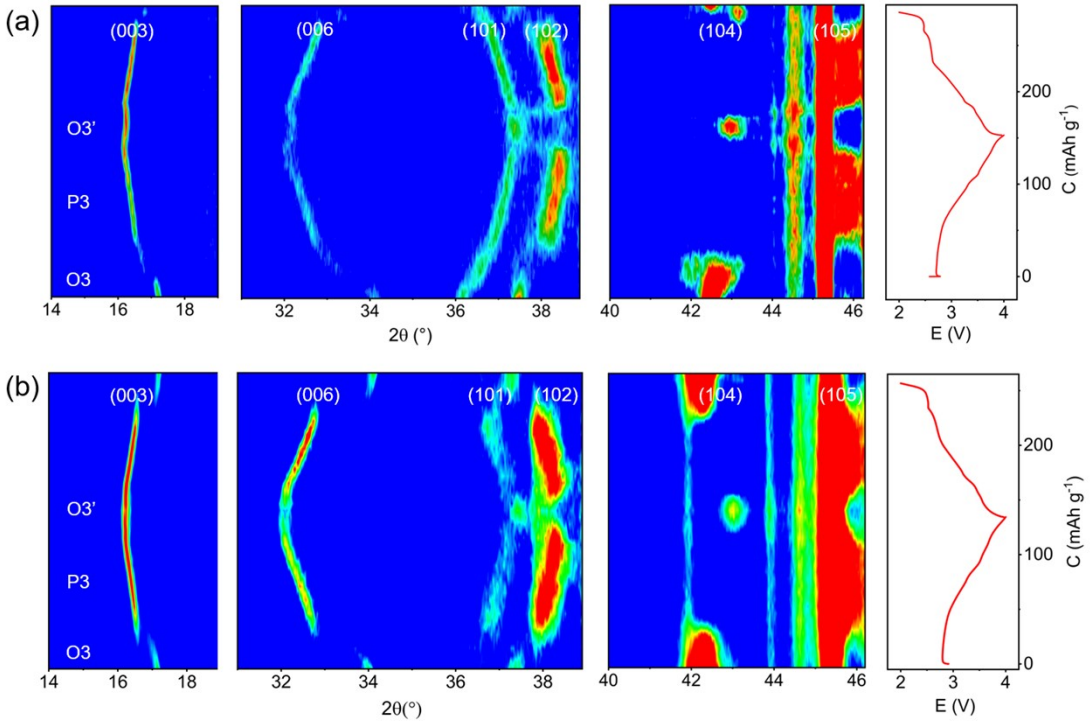

Fig. S9 Contour maps corresponding to *in-situ* XRD of (a) O3-NaNMC and (b) O3-NaNMS.

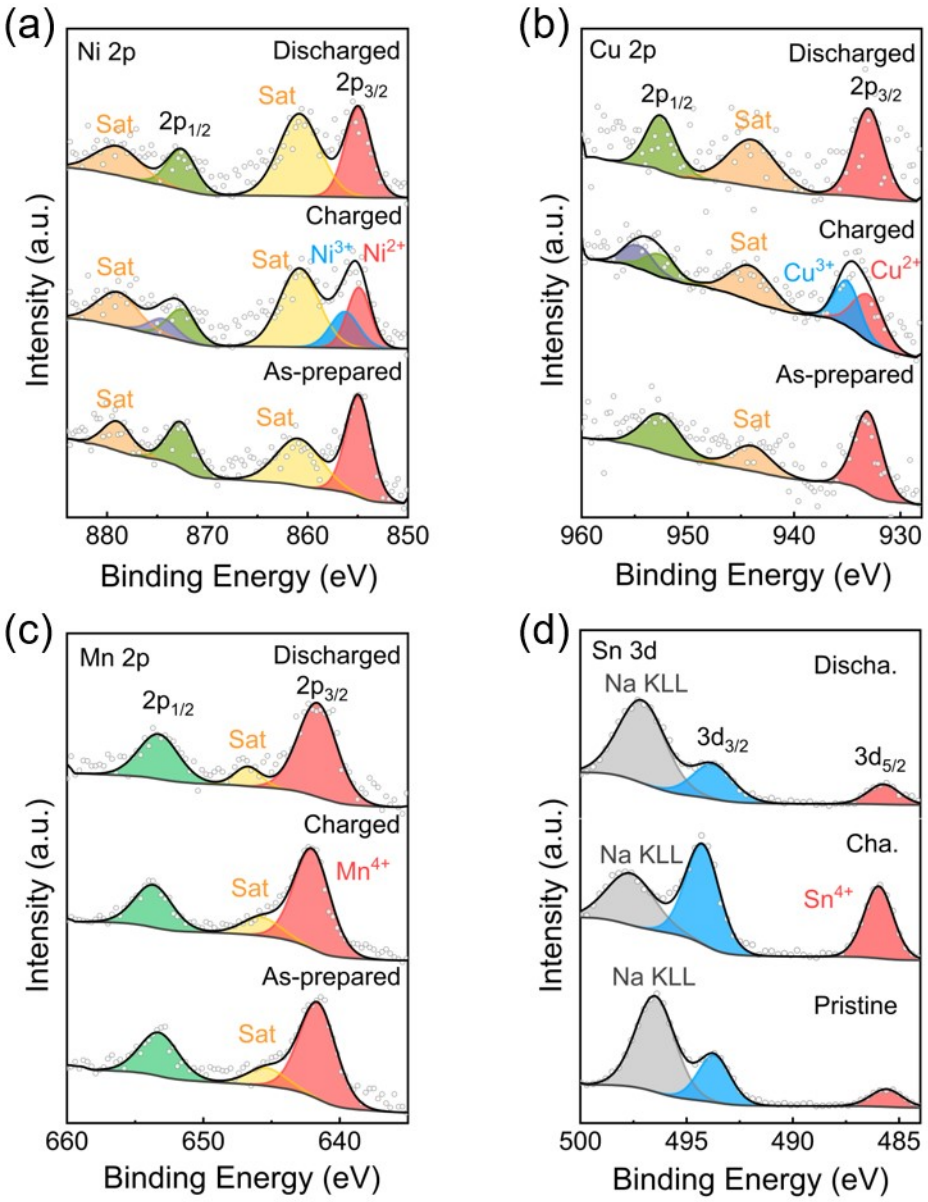

Fig. S10 XPS of (a) Ni 2p, (b) Cu 2p, (c) Mn 2p and (d) Sn 3d collected for pristine and cycled O3-NaNMCS electrodes.

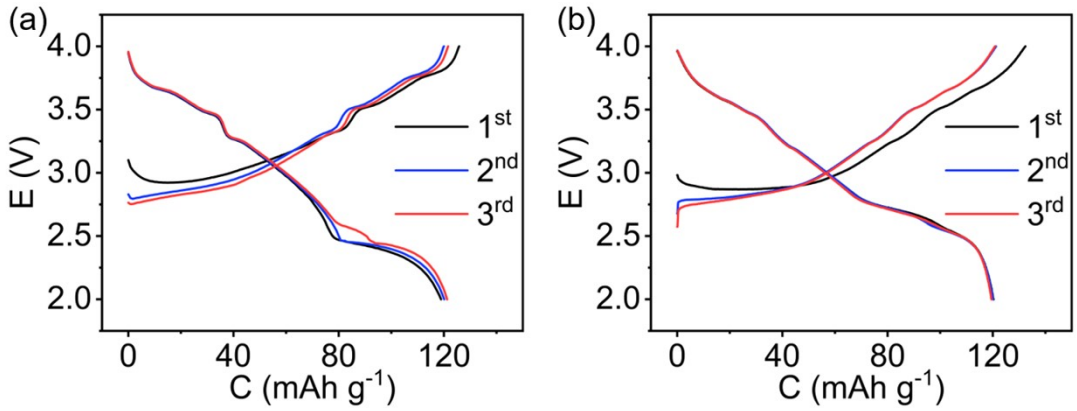

Fig. S11 Charge/discharge curves for initial cycles of (a) O3-NaNMC and (b) O3-NaNMS at a current density of 50 mA g^{-1}.

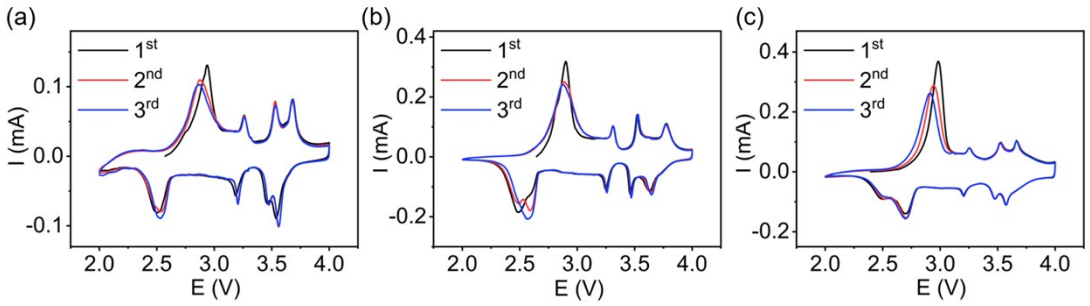

Fig. S12 CV curves of (a) O3-NaNM, (b) O3-NaNMC and (c) O3-NaNMS at 0.1 mV s^{-1}.

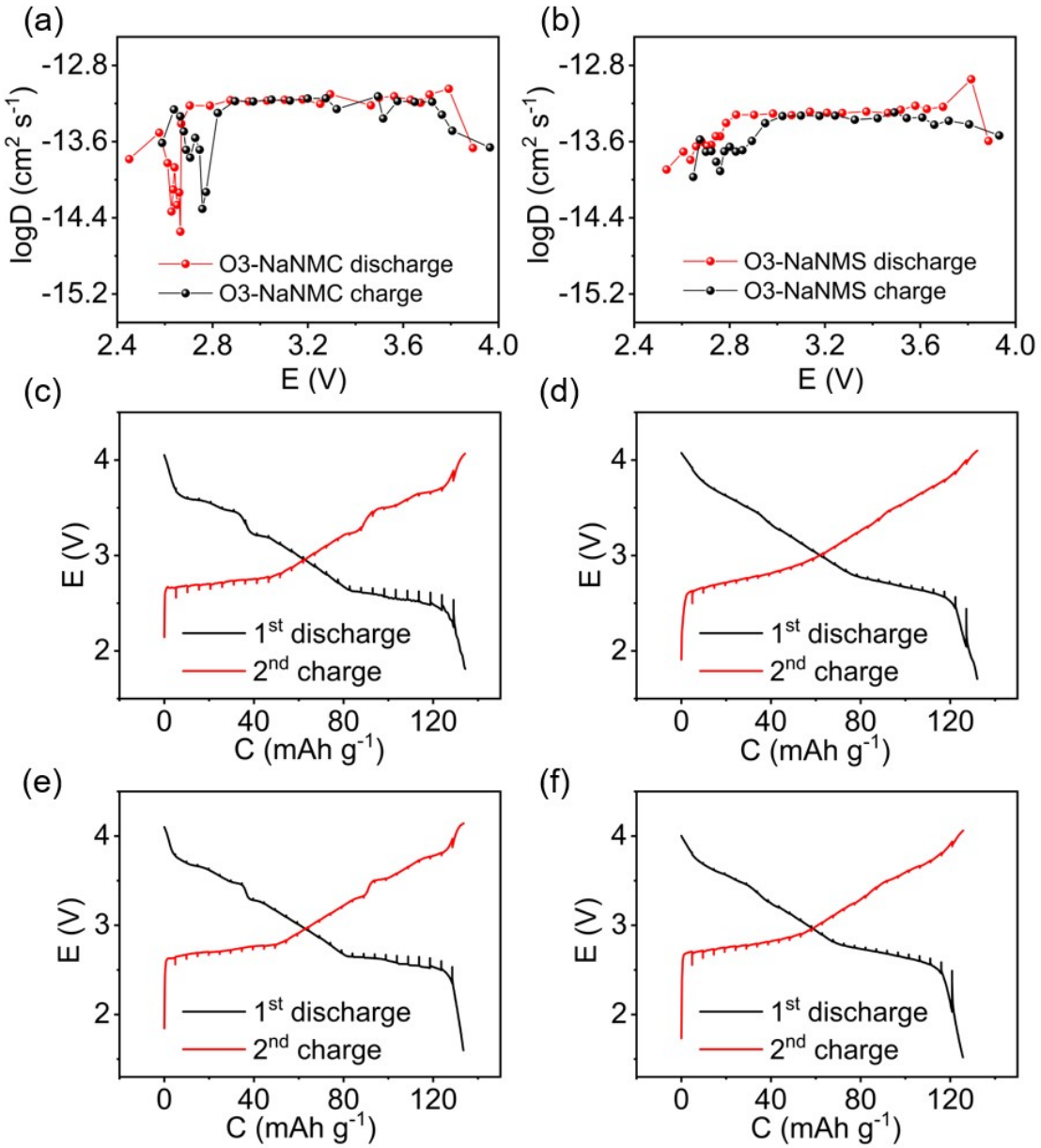

Fig. S13 (a, b) Calculated Na^+ diffusion coefficients of O3-NaNMC and O3-NaNMS. GITT charge/discharge curves of (c) O3-NaNM, (d) O3-NaNMCS, (e) O3-NaNMC and (f) O3-NaNMS between 2.0 and 4.0V at 10 mA g^{-1}.

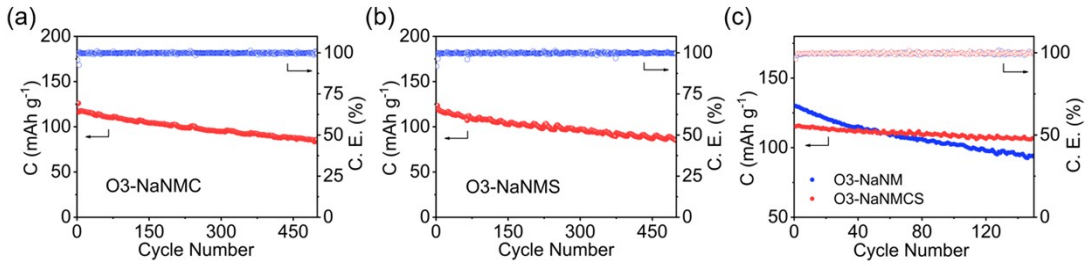

Fig. S14 Cycling performance of (a) O3-NaNMC and (b) O3-NaNMS at 200 mA g^{-1}. (c) Cycling performance of O3-NaNM and O3-NaNMCS at 50 mA g^{-1}.

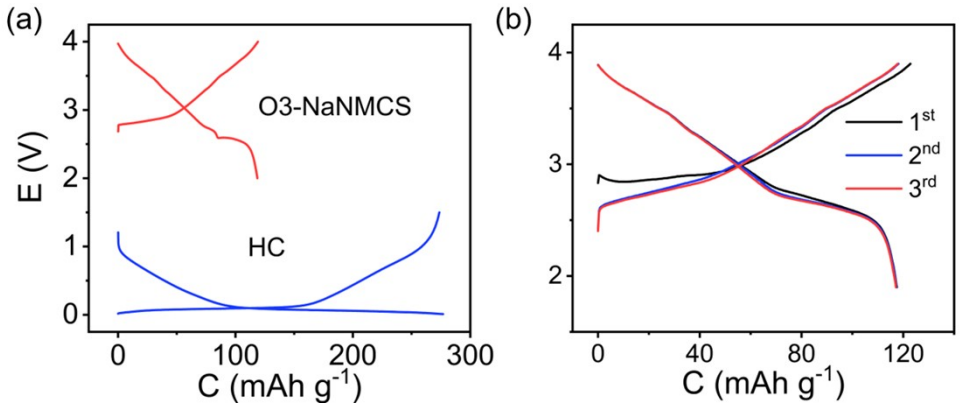

Fig. S15 (a) Typical charge/discharge curves for the 2nd cycle of O3-NaNMCS and HC at 20 mA g^{-1}. (b) Charge and discharge profiles of HC//O3-NaNMCS full cell at 50 mA g^{-1}.

Table S1. ICP-OES results of as-prepared samples.

Theoretical chemical formula	Composition from ICP				
	Na	Mn	Ni	Cu	Sn
$NaNi_{0.50}Mn_{0.50}O_2$	0.993	0.503	0.503	-	-
$NaNi_{0.40}Mn_{0.50}Cu_{0.10}O_2$	0.994	0.482	0.418	0.092	-
$NaNi_{0.50}Mn_{0.45}Sn_{0.05}O_2$	0.998	0.438	0.472	-	0.047
$NaNi_{0.4}Mn_{0.45}Cu_{0.10}Sn_{0.05}O_2$	0.993	0.428	0.382	0.098	0.049

Table S2. Summary of Rietveld refinement results of O3-NaNM.

Sample		$Na_{0.993}Ni_{0.503}Mn_{0.503}O_2$			
Space group		*Rm*			
a [Å] / c [Å]		2.946(5) / 16.049(3)			
Atom	Site			Wyckoff	Occupancy
Na	3a	0	0	0	0.992(8)
Ni	3b	0	0	0.5	0.503
Mn	3b	0	0	0.5	0.503
O	6c	0	0	0.236(7)	1
Reliability factors R_p = 2.16%, R_{wp} = 3.34%					

Table S3. Summary of Rietveld refinement results of O3-NaNMCS.

Sample		$Na_{0.993}Ni_{0.382}Mn_{0.428}Cu_{0.098}Sn_{0.049}O_2$			
Space group		*Rm*			
a [Å] / c [Å]		2.973(9) / 16.023(2)			
Atom	Site			Wyckoff	Occupancy
Na	3a	0	0	0	0.993(2)
Ni	3b	0	0	0.5	0.382
Mn	3b	0	0	0.5	0.428
Cu	3b	0	0	0.5	0.098
Sn	3b	0	0	0.5	0.049
O	6c	0	0	0.240(2)	1
Reliability factors R_p = 3.04%, R_{wp} = 4.39%					

Table S4. Summary of Rietveld refinement results of O3-NaNMC.

Sample		$Na_{0.994}Ni_{0.418}Mn_{0.482}Cu_{0.092}O_2$			
Space group		*Rm*			
a [Å] / c [Å]		2.955(5) / 16.016(3)			
Atom	Site			Wyckoff	Occupancy
Na	3a	0	0	0	0.993(9)
Ni	3b	0	0	0.5	0.418
Mn	3b	0	0	0.5	0.482
Cu	3b	0	0	0.5	0.092
O	6c	0	0	0.236(9)	1
Reliability factors R_p = 2.24%, R_{wp} = 3.13%					

Table S5. Summary of Rietveld refinement results of O3-NaNMS.

Sample		$Na_{0.998}Ni_{0.472}Mn_{0.438}Sn_{0.047}O_2$			
Space group		*Rm*			
a [Å] / c [Å]		2.969(3) / 16.019(1)			
Atom	Site			Wyckoff	Occupancy
Na	3a	0	0	0	0.998(0)
Ni	3b	0	0	0.5	0.472
Mn	3b	0	0	0.5	0.438
Sn	3b	0	0	0.5	0.047
O	6c	0	0	0.240(4)	1
Reliability factors R_p = 2.91%, R_{wp} = 4.53%					

Table S6. Atomic distances, slab thickness, Na layer spacing for as-prepared materials.

Parameters	O3-NaNM	O3-NaNMC	O3-NaNMS	O3-NaNMCS
TM-O (Å)	2.039	2.044	2.083	2.082
TMO_2 (Å)	2.249	2.251	2.363	2.358
Na layer (Å)	3.101	3.088	2.977	2.983
Interslab distance (Å)	5.350	5.339	5.340	5.341

Table S7. Curvefit Parameters[a] for Ni K-edge EXAFS for O3-NaNMCS.

Path	d [b] / Å	N	R / Å	σ^2 / Å^2
Ni-O	2.082	4.6(3)	2.02(1)	0.004(1)
Ni-Ni	2.974	6 [c]	2.86(1)	0.007(0)
Ni-Na	3.175	6 [c]	3.37(2)	0.009(2)

[a] S_0^2 was fixed as 1.0. ΔE_0 was refined as a global fit parameter, returning the value of (-3±1) eV. Data ranges: 2.5 ≤ k≤ 12.5 Å^{-1}, 1.0≤ R ≤ 3.0 Å. The number of variable parameters is 8, out of a total of 12.7 independent data points. R factor for this fit is 0.4 %. [b] The distances for Ni-O, Ni-Ni and Ni-Na are from the crystal structure of O3-NaNMCS. [c] These coordination numbers were constrained as N(Ni-Ni) = 6 and N(Ni-Na) = 6 based on the crystal structure.

Table S8. Curvefit Parameters for Mn K-edge EXAFS for O3-NaNMCS.

Path	d [a] / Å	N	R / Å	σ^2 / Å^2
Mn-O	2.082	4.6(5)	1.93(1)	0.003(1)
Mn-Mn	2.974	6 [b]	2.98(1)	0.004(2)
Mn-Na	3.175	6 [b]	3.10(3)	0.008(4)

S_0^2 for this fit is 0.7. ΔE_0 was refined as a global fit parameter, returning the value of (-4±1) eV. Data ranges: 2.5 ≤ k≤ 11.5 Å^{-1}, 1.0≤ R ≤ 3.0 Å. The number of variable parameters is 9, out of a total of 11.2 independent data points. R factor for this fit is 0.4 %. [a] The distances for Mn-O, Mn-Mn and Mn-Na are from the crystal structure of O3-NaNMCS. [b] These coordination numbers were constrained as N(Mn-Mn) = 6 and N(Mn-Na) = 6 based on the crystal structure.

Table S9. Curvefit Parameters for Ni K-edge EXAFS for O3-NaNM.

Path	d [a] / Å	N	R / Å	σ^2 / Å^2
Ni-O	2.039	6 [b]	2.01(1)	0.005(2)
Ni-Ni	2.946	6 [b]	2.85(1)	0.009(1)
Ni-Na	3.170	6 [b]	3.33(3)	0.006(3)

S_0^2 for this fit is 0.7. ΔE_0 was refined as a global fit parameter, returning the value of (-4±1) eV. Data ranges: 2.5 ≤ k≤ 11.5 Å^{-1}, 1.0≤ R ≤ 3.0 Å. The number of variable parameters is 8, out of a total of 11.2 independent data points. R factor for this fit is 1.2 %. [a] The distances for Ni-O, Ni-Ni and Ni-Na are from the crystal structure of O3-NaNM. [b] These coordination numbers were constrained as N(Ni-O) = 6, N(Ni-Ni) = 6 and N(Ni-Na) = 6 based on the crystal structure.

Table S10. Curvefit Parameters for Mn K-edge EXAFS for O3-NaNM.

Path	d [a] / Å	N	R / Å	σ^2 / Å^2
Mn-O	2.039	6 [b]	1.90(1)	0.003(2)
Mn-Mn	2.946	6 [b]	2.88(1)	0.004(1)[c]
Mn-Na	3.170	6 [b]	2.90(3)	0.004(1)[c]

S_0^2 for this fit is 0.6. ΔE_0 was refined as a global fit parameter, returning the value of (-5±1) eV. Data ranges: $3 \leq k \leq 11.5$ Å^{-1}, $1.0 \leq R \leq 3.0$ Å. The number of variable parameters is 7, out of a total of 10.6 independent data points. R factor for this fit is 0.8 %. [a] The distances for Mn-O, Mn-Mn and Mn-Na are from the crystal structure of O3-NaNM. [b] These coordination numbers were constrained as N(Mn-O) = 6, N(Mn-Mn) = 6 and N(Mn-Na) = 6 based on the crystal structure. [c] The Debye Waller factors were constrained as σ^2(Mn-Mn) = σ^2(Mn-Na) for reducing the number of variables.

Reference

1 M. E. A. El-Mikkawy, A note on a recent paper by J. S. Respondek, *AM*, 2012, **03**, 509–510.

2 K. Momma and F. Izumi, VESTA 3 for three-dimensional visualization of crystal, volumetric and morphology data, *J Appl Cryst*, 2011, **44**, 1272–1276.

3 J. P. Perdew, K. Burke and M. Ernzerhof, Generalized gradient approximation made simple, *Phys. Rev. Lett.*, 1996, **77**, 3865–3868.